

**\*\*Volume Title\*\***

*ASP Conference Series, Vol. \*\*Volume Number\*\**

**\*\*Author\*\***

© **\*\*Copyright Year\*\*** *Astronomical Society of the Pacific*

## Iron Depletion into Dust Grains in Galactic Planetary Nebulae

G. Delgado-Inglada and M. Rodríguez

*Instituto Nacional de Astrofísica, Óptica y Electrónica (INAOE), Apdo Postal 51 y 216, 72000 Puebla, Pue. Mexico*

**Abstract.** We present preliminary results of an analysis of the iron depletion factor into dust grains for a sample of 20 planetary nebulae (PNe) from the Galactic bulge. We compare these results with the ones we obtained in a prior analysis of 28 Galactic disk PNe and 8 Galactic H II regions. We derive high depletion factors in all the objects, suggesting that more than 80% of their iron atoms are condensed into dust grains. The range of iron depletions in the sample PNe covers about two orders of magnitude, and we explore here if the differences are related to the PN morphology. However, we do not find any significant correlation.

### 1. Introduction

Asymptotic giant branch (AGB) stars suffer mass loss episodes during the late stages of their evolution. The combination of high densities with relatively low temperatures makes the atmospheres of these stars favourable sites for grain formation, and in fact they are considered one of the most efficient sources of dust in the Galaxy (see, e.g., Whittet 2003). Planetary nebulae (PNe) are created when AGB stars reach temperatures high enough to ionize the material previously ejected. Several authors have studied the dust present in PNe, but it is not clear how much dust they have and whether it is destroyed or modified during their lifetimes (Pottasch et al. 1984; Lenzuni et al. 1989; Stasińska & Szczerba 1999).

We study the dust in PNe through the analysis of the iron depletion factor, the ratio between the expected abundance of iron and the one measured in the gas phase. The abundances of refractory elements like iron have been calculated from ultraviolet absorption lines in several interstellar clouds toward different sight lines, and the low values obtained, compared to the solar ones, are generally interpreted as due to depletion into dust grains (see, e.g., Morton 1974). Iron is mostly condensed into grains and has a relatively high cosmic abundance. Those two facts together make iron an important contributor to the mass of refractory grains (Sofia et al. 1994), and hence the iron depletion factor is likely to reflect the abundance of refractory elements in dust grains. Besides, in ionized nebulae iron is the refractory element with the strongest lines in the optical range of the spectrum.

In a previous work (Delgado-Inglada et al. 2009), we performed a homogeneous analysis of the iron abundance in a sample of 28 Galactic disk PNe and 8 Galactic H II regions. We obtained very low iron abundances in all the objects, implying that more than 90% of their total iron abundance is condensed into dust grains. This suggests that iron depletes very efficiently in AGB stars and molecular clouds, whereas refractory

dust is barely destroyed in the ionized gas of PNe and H II regions. Here, we extend our analysis to include 20 Galactic bulge PNe (observed by Wang & Liu 2007), and study the dependence of the results on PN morphology.

## 2. The analysis

In H II regions and low ionization PNe,  $\text{Fe}^{++}$  and  $\text{Fe}^{+3}$  are the dominant ionization stages of iron. Due to the faintness of [Fe IV] lines, the gaseous iron abundance is usually calculated from the  $\text{Fe}^{++}$  abundance and an ionization correction factor (ICF) derived from photoionization models. However, for the handful of objects with measurements of [Fe III] and [Fe IV] lines, a discrepancy has been found between the abundance calculated with the aforementioned method and the one found by adding the abundances of  $\text{Fe}^{++}$  and  $\text{Fe}^{+3}$ . Rodríguez & Rubin (2005) studied this discrepancy and derived three correction schemes that take into account what changes in all the atomic data involved in the calculations would solve the discrepancy: 1) a decrease in the collision strengths for  $\text{Fe}^{+3}$  by factors of  $\sim 2-3$ , 2) an increase in the collision strengths for  $\text{Fe}^{++}$  by factors of  $\sim 2-3$ , or 3) an increase in the total recombination coefficient or the rate of the charge-exchange reaction with  $\text{H}^0$  for  $\text{Fe}^{+3}$  by a factor of  $\sim 10$ . Since these three possibilities are equally plausible, and since the discrepancy could be due to some combination of them, the real value of the iron abundance will be intermediate between the extreme values derived with the three correction schemes.

As in our previous work, we select PNe with a relatively low degree of ionization ( $I(\text{He II } \lambda 4686)/I(\text{H}\beta) \lesssim 0.3$ , see Delgado-Inglada et al. 2009), and with moderate electron density (below  $25\,000\text{ cm}^{-3}$ ), since high densities can be associated with large density gradients that introduce large uncertainties in the calculations. Besides, the objects have spectra with all the lines we need to calculate the physical conditions and the abundances of  $\text{Fe}^{++}$ ,  $\text{O}^+$ , and  $\text{O}^{++}$ . We calculate a mean electron density and two electron temperatures (using the usual [N II] and [O III] diagnostic line ratios) for the low and high ionization regions; and with them we derive the  $\text{O}^+$ ,  $\text{O}^{++}$ , and  $\text{Fe}^{++}$  abundances. To derive the total oxygen abundances we use the ICF from Kingsburgh & Barlow (1994) and for iron the three ionization schemes of Rodríguez & Rubin (2005). See Delgado-Inglada et al. (2009) for more details on the procedure and on the atomic data we use. The uncertainties in all the quantities were estimated via Montecarlo simulations (Delgado-Inglada & Rodríguez, in prep.).

## 3. Results

Figure 1 shows the values of the Fe/O abundance ratio (left axis), and the depletion factors (right axis) for Fe/O:  $[\text{Fe}/\text{O}] = \log(\text{Fe}/\text{O}) - \log(\text{Fe}/\text{O})_\odot$ . We use the solar abundance from Lodders 2003,  $\log(\text{Fe}/\text{O})_\odot = -1.22 \pm 0.06$ , as the expected total abundance. Filled symbols in this figure indicate the values derived using the correction scheme defined by point (3) above, while empty symbols represent the values obtained with the other two correction schemes. The real values are expected to be in the range defined by these three values. We find that both PNe and H II regions have consistently high depletion factors, with more than 80% of their iron atoms condensed into dust grains. The differences between the Fe/O values derived with the three correction schemes depend on the degree of ionization of the objects: the higher the degree of ionization, the

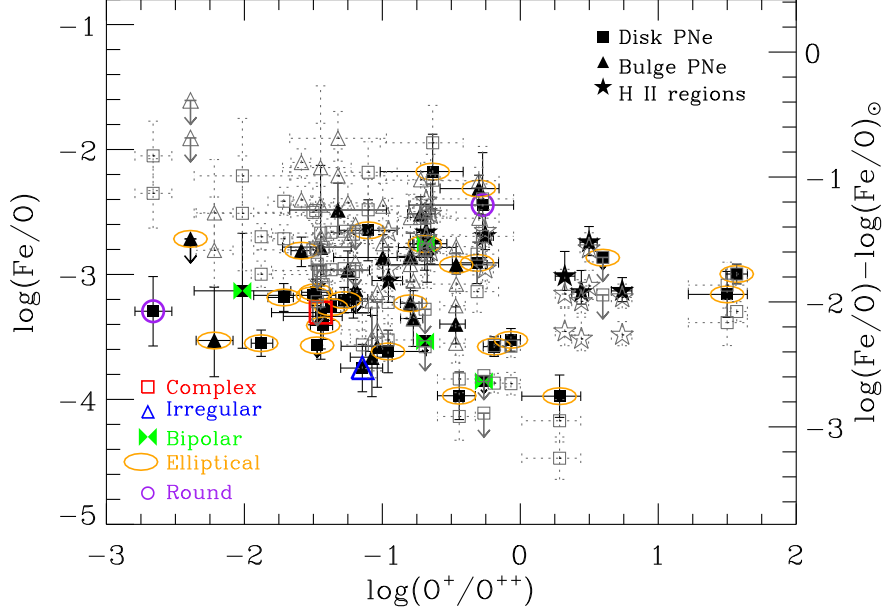


Figure 1. Values of Fe/O (left axis) and the depletion factors for Fe/O ( $[\text{Fe}/\text{O}] = \log(\text{Fe}/\text{O}) - \log(\text{Fe}/\text{O})_{\odot}$ , right axis) as a function of the degree of ionization. Three values of Fe/O are shown for each object, derived using the three correction schemes of Rodríguez & Rubin (2005). The PNe are classified according to their origin (disk or bulge) and their morphology. See the text for more explanations.

greater the difference in Fe/O values. Hence, the iron abundance is better constrained for the objects with  $\log(\text{O}^+/\text{O}^{++}) \gtrsim -1.0$ , where the differences between the correction schemes are  $\leq 0.5$  dex. No matter which correction scheme we consider, the range of depletions is wide in this region, with a difference in the iron abundance of a factor of  $\sim 100$  between the objects with the lowest and the highest value. Although these variations should be reflecting real differences between the objects, we do not find any clear correlation between the iron abundances and parameters related to the nebular age (such as the electron density or the surface brightness of the PN) or with the dust chemistry (Delgado-Inglada & Rodríguez, in prep.). The first result suggests that no significant destruction of dust grains is taking place in these objects, and the second one argues for a similar efficiency of iron depletion in C-rich and O-rich environments.

Here, we explore the relation between the iron abundances of the sample PNe and their morphological types. There is some observational evidence that the morphological type of a PN is related to the progenitor mass. Symmetric PNe (round or elliptical nebulae) might descend from low mass progenitors, and asymmetric PNe (bipolar or more complex objects) might have the most massive progenitor stars (see, e.g., Corradi & Schwarz 1995; Stanghellini et al. 2006). Asymmetric PNe have also been associated with binary systems (see, e.g., Corradi & Schwarz 1995; Soker 1998; de Marco 2009), and with stellar rotation and/or magnetic fields (see, e.g., García-Segura et al. 1999). Although the reasons behind the shaping of PNe are still matter of debate, we

study here if there is a correlation between the morphologies and the iron depletion factors. Figure 1 shows the PNe morphologies given by the Planetary Nebula Image Catalog of Bruce Balick (PNIC<sup>1</sup>) and by Stanghellini et al. (2002) for the 34 objects with available images. Two of them are classified as round, 26 as elliptical, four as bipolar, one as irregular, and one more as complex. This figure shows that there is no obvious trend relating the morphological type and the amount of iron condensed in dust grains. For example, elliptical and bipolar PNe are distributed in the whole range of depletions. The three correction schemes used in the abundance determination give consistent results on this issue.

#### 4. Conclusions

We derive the iron abundance in a sample of 20 Galactic bulge PNe, and compare the results with the ones previously obtained for 28 Galactic disk PNe and 8 Galactic H II regions. We find high depletion factors in all the objects: less than 20% of their expected total number of iron atoms are measured in the gas phase. This result suggests that iron depletion into dust grains is an efficient process in AGB stars, whereas dust destruction is not very efficient in the subsequent PN phase. Although the range of depletions in the sample PNe is wide, covering around two orders of magnitude, we do not find any correlation between the iron depletion factors and the morphology of the PNe. Further details of the analysis will be presented in Delgado-Inglada & Rodríguez (in prep.).

**Acknowledgments.** We acknowledge support from Mexican CONACYT project 50359-F.

#### References

- Corradi, R. L. M., & Schwarz, H. E. 1995, *A&A*, 293, 871  
 de Marco, O. 2009, *PASP*, 121, 316  
 Delgado-Inglada, G., Rodríguez, M., Mampaso, A., & Viironen, K. 2009, *ApJ*, 694, 1335  
 García-Segura, G., Langer, N., Różyczka, M., & Franco, J. 1999, *ApJ*, 517, 767  
 Kingsburgh, R. L., & Barlow, M. J. 1994, *MNRAS*, 271, 257  
 Lenzuni, P., Natta, A., & Panagia, N. 1989, *ApJ*, 345, 306  
 Lodders, K. 2003, *ApJ*, 591, 1220  
 Morton, D. C. 1974, *ApJ*, 193, 35  
 Pottasch, S. R., Baud, B., Beintema, D., Emerson, J., Harris, S., Habing, H. J., Houck, J., Jennings, R., & Marsden, P. 1984, *A&A*, 138, 10  
 Rodríguez, M., & Rubin, R. H. 2005, *ApJ*, 626, 900  
 Sofia, U. J., Cardelli, J. A., & Savage, B. D. 1994, *ApJ*, 430, 650  
 Soker, N. 1998, *ApJ*, 496, 833  
 Stanghellini, L., Guerrero, M. A., Cunha, K., Manchado, A., & Villaver, E. 2006, *ApJ*, 651, 898  
 Stanghellini, L., Villaver, E., Manchado, A., & Guerrero, M. 2002, *ApJ*, 576, 285  
 Stasińska, G., & Szczerba, R. 1999, *A&A*, 352, 297  
 Wang, W., & Liu, X.-W. 2007, *MNRAS*, 381, 669  
 Whittet, D. C. B. 2003, *Dust in the Galactic Environment* (Bristol:IoP), 2nd ed.

---

<sup>1</sup><http://www.astro.washington.edu/users/balick/PNIC/>